Decoupled-Control Method of Normal and Thrust Forces in SLIM Maglev Vehicle ME01

Yoshida, Kinjiro
Department of Electrical and Electronic Systems Engineering, Graduate School of Information Science and Electrical Engineering, Kyushu University

Shi, Liming
Department of Electrical and Electronic Systems Engineering, Kyushu University : Graduate Student | Yasukawa Co.

Yoshida, Takashi
Department of Electrical and Electronic Systems Engineering, Graduate School of Information Science and Electrical Engineering, Kyushu University : Graduate Student

https://doi.org/10.15017/1513714

出版情報：九州大学大学院システム情報科学紀要. 5 (1), pp.37-42, 2000-03-24. 九州大学大学院システム情報科学研究院
バージョン：
権利関係：

九州大学大学院
システム情報科学研究科報告
第5巻 第1号 平成12年3月

Research Reports on Information Science and
Electrical Engineering of Kyushu University
Vol.5, No.1, March 2000

Decoupled-Control Method of Normal and Thrust Forces in SLIM Maglev Vehicle ME01

Kinjiro YOSHIDA*, Liming SHI** and Takashi YOSHIDA***

(Received December 10, 1999)

Abstract: This paper proposes a decoupled-control method of normal and thrust forces in single-sided linear induction motor (SLIM) which is based on a unified concept of machine principle. This method is derived from the analytical formulas for normal and thrust forces of a SLIM. This method can be applied to a LIM vehicle system, in which the normal force is used to levitate and the thrust force to propel a LIM vehicle without force-couple of LIM. By using this method, a compact combined levitation-and-propulsion system with LIM only can be realized. This method is verified by a successful simulation of levitation and propulsion for a SLIM model vehicle ME01 running under water in our Laboratory.

Keywords: LIM, Normal and thrust forces, Decoupled-control, Magnetic levitation-and-propulsion

1. Introduction

A concept of combined magnetic levitation-and-propulsion with only a linear synchronous motor (LSM)[1,2] has been realized successfully without any additional magnets for levitation[3,4]. One of the keys is the decoupled-control method due to the lift and thrust forces of a LSM[5-8]. It is well known that linear induction motor (LIM) is much simpler in construction, its maintenance is easier and the cost is much lower than LSM. So LIM is often applied to transportation system and magnetic levitation (Maglev) system as a no-contacting driving source[9]. But because the normal force of LIM varies depending strongly on the vehicle speed and applied frequency, this force is generally seldom utilized in transportation systems and its effect is always restrained as far as possible. When the normal force of a LIM can be utilized actively as a lift force to support effectively a transportation vehicle, a very compact and low cost combined levitation-and-propulsion system with only LIM has been realized under the water by the help of water buoyancy[10].

This paper proposes a decoupled-control method of normal and thrust forces in single-sided LIM, which is derived from the view point of a unified concept for machine principle. This method can be applied in a control system of a LIM vehicle. Based on this method, the normal force is used to levitate the vehicle and the thrust force to propel the vehicle without coupling between the normal and thrust forces of the LIM. The method is derived from the analytical formulas for normal and thrust forces in the SLIM with no secondary back-iron using space harmonic analysis method[11,12]. The effective value of armature-current and slip-frequency are calculated according to the command normal and thrust forces obtained from the optimal servo control theory. The normal force is repulsive in a SLIM without secondary back-iron used in this study. Proposed decoupled-control method has been verified by a control simulation of repulsive-mode levitation-propulsion for a short secondary SLIM Maglev model vehicle ME01.

ME01 is the first model vehicle of Marine-Express Project, of which the basic concept is a unique amphibious linear motor vehicle able to run both on land and underwater initiated by our University in 1989[10]. ME01 is designed and manufactured to run using only one short-secondary SLIM along the canned linear motor guide way in a 6-m long water tank in our Laboratory.

2. Decoupled Control of Normal and Thrust Forces

Fig. 1 shows the analysis model of a SLIM without secondary back-iron. This model can be analyzed by space harmonic analysis method which was developed in[12]. This method proposed a precious theoretical analysis of LIM, in which the end effects of LIM is taken into account effectively and the normal force

* Department of Electrical and Electronic Systems Engineering
** Department of Electrical and Electronic Systems Engineering, Graduate Student (At present; Yasukawa Co.)
*** Department of Electrical and Electronic Systems Engineering, Graduate Student

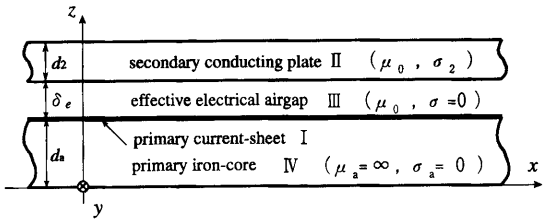

Fig. 1 Analysis model of SLIM without secondary back-iron.

and thrust force can be also calculated length δ=1.5 mm and the effective value of armature current I_1=1 A. It is clear that the normal force F_z is always positive and repulsive-mode levitation is possible. **Fig. 3** shows how the F_x/F_z depends on only the slip-frequency sf of the SLIM with no secondary back-iron. Here, the transverse edge effects are considered as the end-ring resistance in overhang-region of the secondary conducting sheet[13]. **Fig. 3** means that a slip-frequency sf can be determined uniquely from one variable F_x/F_z. F_x is the propulsion force in the moro-running region and the breaking force in the regenerative-and inverse-phase-breaking regions. Because F_z is always positive, **Fig. 3** is thus applicable to these all three running regions by considering negative slip in the regenerative-breaking region. It is an important characteristic to realize a decoupled control of F_x and F_z. Because there is no back-iron in the secondary here, repulsive normal force is obtained to support the vehicle with the secondary conducting plate underneath. For an attractive-mode levitation, to obtain the attractive normal-force the back-iron is evidently necessary. A SLIM is to be designed meticulously considering greatly the requirement for normal force.

Fig. 4 shows the block diagram of the decoupled control of the normal and thrust forces in SLIM. According to the optimal robust servo control theory, command normal force F_z^* and thrust force F_x^* are determined to control the vehicle following quickly the demand patterns of position x_0, speed numerically but easily. In this paper, to derive an analytical formula for decoupled-control of normal and thrust forces, the short-stator end effects is neglected and only fundamental forward-travelling current is considered.

Especially, in ME01 with short-secondary SLIM, because the copper-secondary length $l_2=p\tau$, which is given in **Table 1**, is very large and the speed is very low, it is reasonable to neglect the short-secondary end effects.

The airgap flux density components B_{x1}^{III} and B_{z1}^{III} at the surface of the primary core are obtained as follows:

$$B_{x1}^{\mathrm{III}}=\left[-\frac{\partial A_y^{\mathrm{III}}}{\partial z}\right]_{z=d_a}=-2\sqrt{2}\ mI_1\frac{k_{w1}N_{ph}}{p\tau}\mu_0 e^{-j\frac{\pi}{\tau}x}e^{j\omega_1 t} \tag{1}$$

$$B_{z1}^{\mathrm{III}}=\left[-\frac{\partial A_y^{\mathrm{III}}}{\partial x}\right]_{z=d_a}=-j2\sqrt{2}\ mI_1\frac{k_{w1}N_{ph}}{p\tau}\mu_0 K_H e^{-j\frac{\pi}{\tau}x}e^{j\omega_1 t} \tag{2}$$

where

$$K_H=\frac{1+\tanh\frac{\pi}{\tau}\delta\cdot\lambda_2\tanh\frac{\pi}{\tau}d_2\lambda_2}{\tanh\frac{\pi}{\tau}\delta+\lambda_2\tanh\frac{\pi}{\tau}d_2\lambda_2}=K_{Hr}+jK_{Hi}=Ke^{j\theta^*} \tag{3}$$

and

$$\lambda_2=\alpha_2+j\beta_2$$

$$\alpha_2=\frac{1}{\sqrt{2}}\sqrt{\sqrt{1+K_{\sigma\mu}(sf)^2}+1} \tag{4}$$

$$\beta_2=\frac{1}{\sqrt{2}}\sqrt{\sqrt{1+K_{\sigma\mu}(sf)^2}-1} \tag{5}$$

where

$$K_{\sigma\mu}=4(\sigma_2\mu_0\tau^2/\pi)^2 \tag{6}$$

I_1 is the effective-value of armature phase current, sf the slip-frequency, s the slip, f the frequency of power source, δ the airgap length, δ_e the effective airgap-length modified by Carter's coefficient, μ_0 the permeability of air. Other parameters are listed in **Table 1**.

The expression for the total normal force F_z and the total thrust force F_x are derived in the following form using the concept of Maxwell's magnetic stresses.

$$\begin{aligned}F_z=F_z^{\mathrm{IV}}&=\frac{1}{2}\left(\frac{1}{2\mu_0}B_{z1}^{\mathrm{III}}B_{z1}^{\mathrm{III}*}-\frac{1}{2\mu_0}B_{x1}^{\mathrm{III}}B_{x1}^{\mathrm{III}*}\right)hp\tau\\&=\frac{hp\tau}{4\mu_0}\left[\left(2\sqrt{2}\ mI_1\frac{k_{w1}N_{ph}}{p\tau}\mu_0 K\right)^2-\left(2\sqrt{2}\ mI_1\frac{k_{w1}N_{ph}}{p\tau}\mu_0\right)^2\right]\\&=\frac{2h\mu_0 m^2I_1^2K_w^2N_{ph}^2}{p\tau}(K^2-1)\end{aligned} \tag{7}$$

$$\begin{aligned}F_x=F_x^{\mathrm{IV}}&=\mathrm{Re}\left(\frac{1}{2\mu_0}B_{x1}^{\mathrm{III}}B_{z1}^{\mathrm{III}*}\right)hp\tau\\&=\frac{ph\tau}{2\mu_0}\mathrm{Re}\left(-2\sqrt{2}\ mI_1\frac{k_{w1}N_{ph}}{p\tau}\mu_0 e^{-j\frac{\pi}{\tau}x}e^{j\omega_1 t}\cdot 2\sqrt{2}\ mI_1\frac{k_{w1}N_{ph}}{p\tau}\mu_0 e^{j\frac{\pi}{\tau}x}e^{-j\omega_1 t}e^{j\frac{\pi}{2}}K_H^*\right)\\&=4\mu_0 h\frac{m^2I_1^2k_{w1}^2N_{ph}^2}{p\tau}\mathrm{Re}(-jk_H^*)\end{aligned} \tag{8}$$

where h is the width of primary iron-core.

Considering F_x/F_z as a parameter in the analysis to a SLIM with no secondary back-iron, this parameter can be derived as a function of only one variable sf as follows.

$$\frac{F_x}{F_z}=\frac{\frac{1}{2\mu_0}\mathrm{Re}(B_{x1}^{\mathrm{III}}B_{z1}^{\mathrm{III}*})hp\tau}{\frac{1}{2}\frac{1}{2\mu_0}(B_{z1}^{\mathrm{III}}B_{z1}^{\mathrm{III}*}-B_{x1}^{\mathrm{III}}B_{x1}^{\mathrm{III}*})hp\tau}$$
$$=2\mathrm{Re}\left(\frac{1}{jK_H-1/(jK_H)^*}\right) \quad (9)$$

Placing (3), (4) and (5) into (9), then F_x/F_z can be explicitly written as

$$F_x/F_z=f(sf) \quad (10)$$

Table 1 gives the specification of the short secondary SLIM used in the LM underwater car ME01 in our Laboratory. **Fig. 2** indicates the dependence of normal force F_z and thrust force F_x of ME01 on slip-frequency sf with that the airgap v_{x0} and airgap-length δ_0 by the feedback of vehicle position x, speed v and airgap-length δ of LIM. To achieve simultaneously the objects of good system response and robust feedback properties, a control system with a two-degree-of-freedom is included in the control law. Command slip-frequency sf^* is calculated by an interpolation from the normal force F_z^* and thrust force F_x^* based on the **Fig. 3** obtained from (10). Then the command effective value of armature-current I_1^* can be calculated from F_x^*, sf^* and demand airgap length δ_0, as follows[14]:

$$I_1^*=f(F_x^*,\ sf^*,\ \delta_0) \quad (11)$$

Table 1 Specification of the experimental single-sided short-secondary LIM for ME01

Item	Symbol	Value
Number of phase	m	3
Number of pole	p	15
Pole pitch	τ	44.7mm
Width of primary iron-core	h	12mm
Number of slots per pole-phase	q	1
Turns per phase	N_{ph}	2625
Winding coefficient	k_{w1}	0.99815
Airgap-length	δ	1.5mm
Thickness of copper secondary	d_2	5.0mm
Width of copper secondary	w_2	30mm
Length of copper secondary	l_2	670.5mm
Resistivity of copper secondary	$1/\sigma_2$	$1.72\times10^{-8}\ \Omega\cdot$m (at 20°)

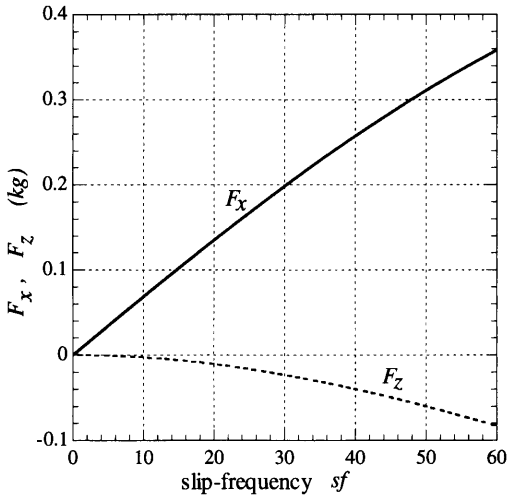

Fig. 2 Dependence of thrust force F_x and normal force F_z on slip-frequency sf.

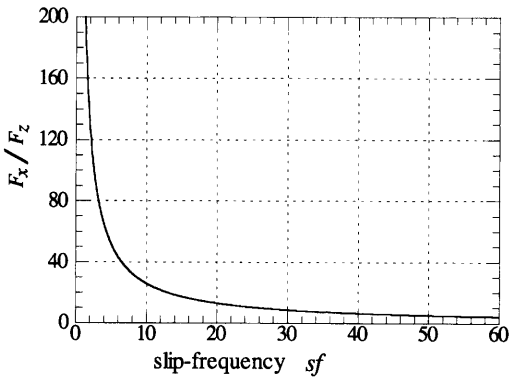

Fig. 3 Dependence of F_x/F_z on slip-frequency sf.

In addition, the command frequency f^* can be also determined easily considering the vehicle speed v. That is to say, for arbitrary F_z^* and F_x^* which are possible for the SLIM, the I_1^* and f^* can be determined uniquely and the vehicle can be levitated by normal force and propelled by thrust force in SLIM. To decelerate the vehicle, regenerative and/or inverse-phase breaking of LIM can be adopted.

3. Levitation-Propulsion Control of ME01

Fig. 5 shows the 1/25-th scale model vehicle ME01 running underwater in a water-tank[10]. **Fig. 6** show its outline structure. ME01 is 95.05cm long, 6.5kg in weight, 12cm in diameter and streamlined with dorsal and tail fines as shown in **Fig. 5**. To sustain at rest and limit the vehicle, upper and lower guide-rollers in the vertical direction and the side guide-rollers in the lateral direction on each side are installed. The LM guide way in the water tank is made of stainless steel and the LM armature-coils of long-stator is filled in the stainless guide way and canned. The vehicle is

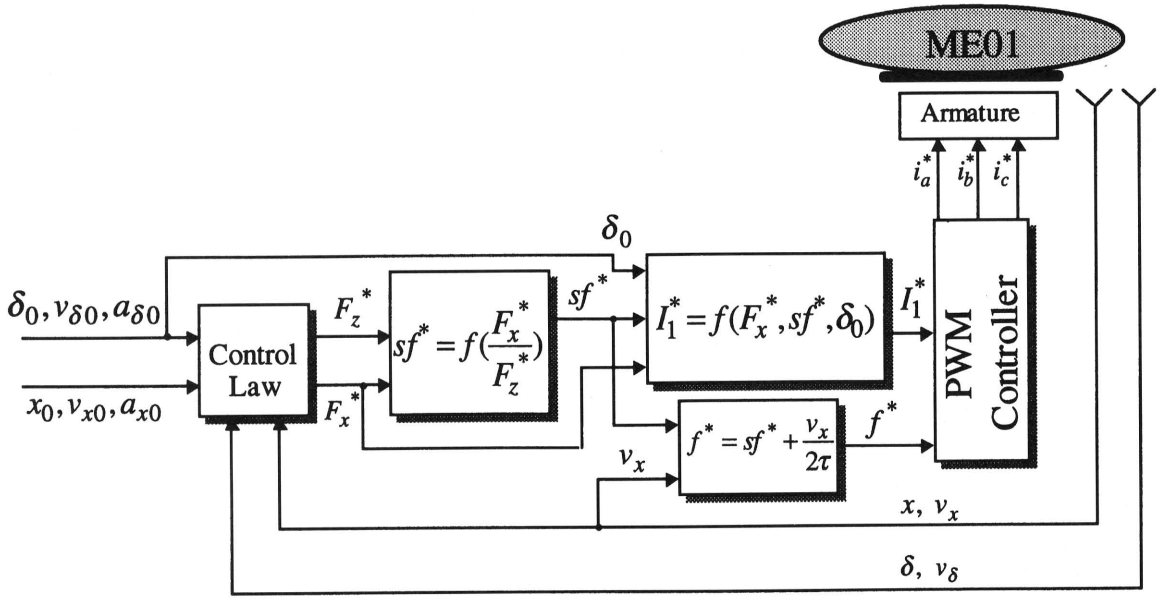

Fig. 4 Block diagram of decoupled-control system of SLIM.

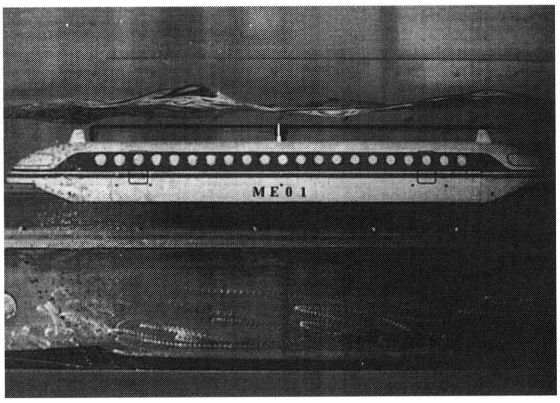

Fig. 5 ME01 running underwater in a water tank.

only fitted with a simple copper plate as a secondary reaction-plate underneath the vehicle. So, the repulsive-mode normal force can be obtained.

The first author has realized successfully a underwater propulsion-control experiment of ME01 in a levitation state[10]. To implement a stable underwater combined levitation-propulsion control, a decoupled-control of normal and thrust forces are necessary. In this paper, a dynamic control simulation of repulsive-mode combined levitation-and-propulsion is carried out based on the proposed decoupled-control method above by using MS-Visual language.

In the simulation, an initial airgap-length is 1mm with the upper guide-rollers contacting on the guide way and the water buoyancy is 0.999 times the vehicle weight. Large buoyancy of water is made use of to lift the vehicle. This buoyancy is supposed as a constant disturbance in the control strategy. The vehicle was accelerated at 0.3m/s^2 with being levitated from 1mm to 1.5mm of airgap-length. Then it ran at a constant speed of 0.6m/s. Finally it was decelerated at -0.3m/s^2 and then stopped. The total running distance is 4.8m. The levitation is started and ended simultaneously with propulsion.

Fig. 7 gives the dynamic simulation results of combined levitation-propulsion of ME01. As shown in **Fig. 7** (a), (b) and (c), vehicle position, speed and (c), vehicle position, speed and airgap-length were controlled to follow the demand patterns x_0, v_{x0} and δ_0

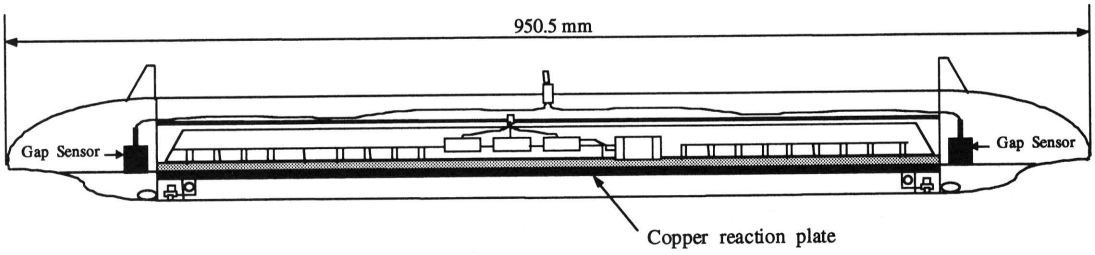

Fig. 6 Decoupled-Control Method of Normal and Thrust Forces in Linear Induction Motor for Maglev Vehicle Marine-Express ME01.

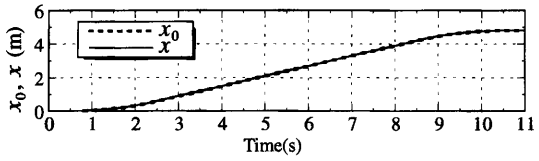

(a) Demand and simulated vehicle-positions

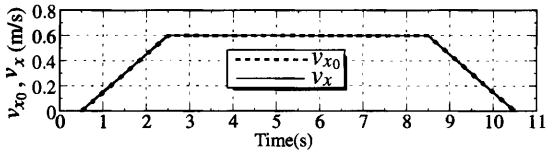

(b) Demand and simulated vehicle-speeds

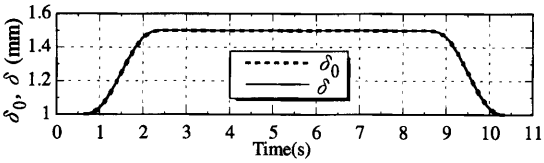

(c) Demand and simulated airgap-lengths

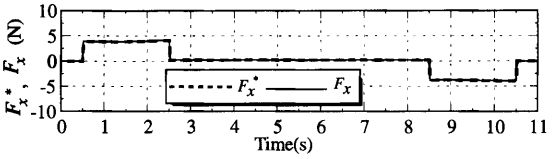

(d) Command and simulated thrust forces

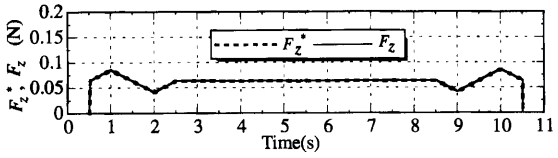

(e) Command and simulated lift forces

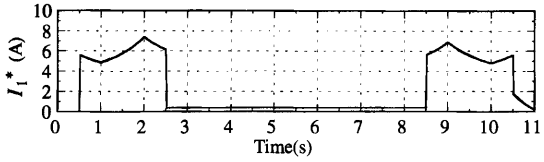

(f) Command effective value of armature-current

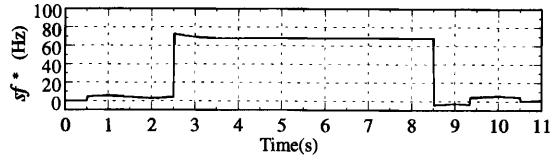

(g) Command slip-frequency

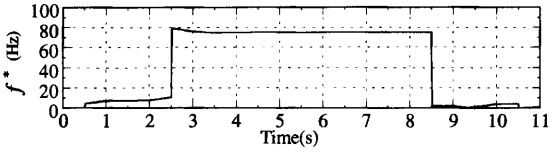

(h) Command frequency

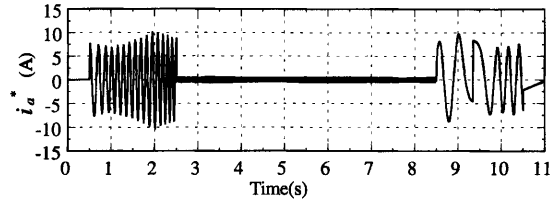

(i) Instantaneous current of a-phase

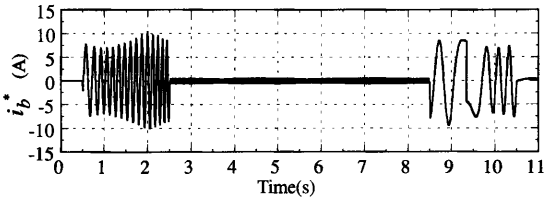

(j) Instantaneous current of b-phase

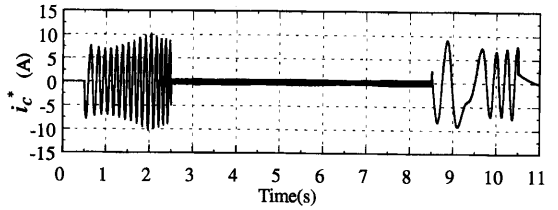

(k) Instantaneous current of c-phase

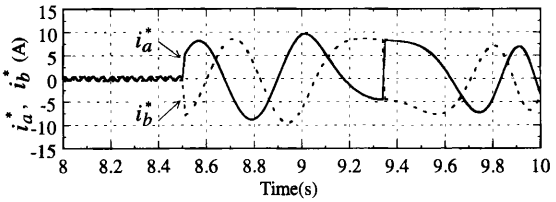

(l) Instantaneous current of a-phase and b-phase in extended time axis

Fig. 7 Simulation result of combined levitation-propulsion in repulsive-mode for ME01 running-underwater.

very well. **Fig. 6** (d) and (e) give the command left force F_z^* and thrust force F_x^* which varied together with the vehicle motion patterns. **Fig. 7** (f), (g) and (h) show the effective-value of armature-current I_1^*, frequency f^* and slip-frequency sf^* corresponding to the levitation and propulsion motion, respectively. The vehicle was accelerated from 0.5s to 2.5s and decelerated from 8.5s to 10.5s. From 2.5s to 8.5s, the vehicle ran at constant low-speed and very small thrust force was required to compensate for only the water resistance, so that the F_x/F_z was small which results in the large value of sf^* as known in **Fig. 3**.

In this simulation, to decelerate the vehicle, first the regenerative breaking was used and then the inverse-phase breaking was applied to stop the vehicle. The phase-exchange happened at an instant about 9.34s, where the frequency is about 0Hz. **Fig. 7** (i), (j) and (k) indicate the instantaneous values of *a*-, *b*- and *c*-phase currents. **Fig. 7** (l) gives the instantaneous values of *a*- and *b*-phase currents in extended time axis to illustrate the phase-exchange point of the two phases.

From these results, it is distinct that the ME01 vehicle was controlled satisfactorily to follow the levitation and propulsion patterns by only SLIM.

4. Conclusions

In this study on SLIM without secondary back-iron, the following results have been obtained:

(1) An analytical formula for the ratio F_x/F_z can be derived as a function of only slip-frequency sf.

(2) On the basis of the above result (1), the decoupled-control method can be obtained for the levitation and thrust forces required to control SLIM Maglev vehicle.

(3) The decoupled-control system is also proposed for the SLIM Maglev vehicle to follow the demand position and speed patterns.

(4) A dynamics simulation of levitation-propulsion in repulsive-mode of ME01 has verified numerically the decoupled-control method proposed here.

References

1) K. Yoshida, "Linear Synchronous Motor Propulsion Method for Guided Vehicle", *Japanese Patent Publication*, No. 1991-27703.

2) K. Yoshida, "Magnetic Levitation and Linear Motor", *Science of Machine*, Vol. 42, No. 4, 1990, pp. 468-474.

3) K. Yoshida, H. Takami, N. Shigemi, Y. Nagano and A. Sonoda, "Repulsive-Mode Levitation and Propulsion Control of a Land Travelling Marine-Express Model Train ME03", *Proceedings of the First International Symposium on Linear Drives for Industry Applications*, Nagasaki, 1995, pp. 41-44.

4) K. Yoshida, H. Takami, Y. Nagano and A. Sonoda, "A New Combined Levitation and Propulsion Control in Repulsive-Mode of a Land Travelling Marine-Express Model Train ME03", *Proceedings of International Conference on Electrical Machines, Spain*, 1996, pp. 242-247.

5) K. Yoshida, S. Nagao, "Levitation and Propulsion Control Simulation of Regardless-of-Speed Superconducting LSM Repulsive Maglev Vehicle", *Proceedings of the 3rd Electromagnetics Symposium, Japan*, 1991, pp. 201-206.

6) K. Yoshida, T. Ohsashi, K. Shiraishi and H. Takami, "Feasibility of Superconducting LSM Rocket Launcher System", *Proceedings of the Second International Symposium on Magnetic Suspension Technology*, Seattle, U. S.A., 1994, pp. 607-621.

7) K. Yoshida, H. Takami, C. Jozaki and S. Kinoshita, "Ultra-Low-Speed Experiments of Combined Levitation-and-Propulsion in PM LSM Controlled-Repulsive Maglev Model Vehicle", *1998 National Convention Record I.E.E., Japan*, 1998, pp. 337-340.

8) K. Yoshida, H. Takami and L. Shi, "Decoupled-Control of Levitation and Propulsion in Underwater LM car ME02", *the Journal of Mathematics and Computers in Simulation*, Vol. 46, 1998, pp. 239-256.

9) The Linear Motor Analysis Methods Technical Committee of IEE, Japan: "The Current State and Future Prospect of Linear Motor Analytical Method", *The Technical Report of IEE, Japan*, Vol. 2, No. 440, 1992.

10) K. Yoshida, H. Muta and N. Teshima, "Underwater Linear Motor Car", *Journal of Applied Electromagnetics in Materials*, No. 2, 1991, pp. 275-280.

11) K. Yoshida and S. Nonaka, "Levitation Forces in Single-Sided Linear Induction Motors for High-speed Ground Transport", *IEEE Transactions on Magnetics*, Vol. MAG-11, NO. 6, Nov. 1975, pp. 1717-1719.

12) K. Yoshida, "A Study on Linear Induction Motor", *Doctoral Dissertation, Kyushu University*, March, 1974.

13) E. R. Laithwaite, D. Tipping and D. E. Hesmondhalgh, "The Application of linear Induction Motor to Conveyors", *Proceedings of IEE*, 107A, 6, 1960, pp. 284-294.

14) K. Yoshida, L. Shi and T. Yoshida, "A decoupled-control of LIM model vehicle ME01 and its levitation-propulsion simulation", *Record of 1998 Joint Conference of Electrical and Electronics Engineering in Kyushu*, No. 1348, 1998.